Pergamon

0022-3697(94)00150-2

J. Phys. Chem. Solids Vol. 56, No. 1, pp. 141–150, 1995

0022-3697/95 $9.50 + 0.00

STRUCTURAL STUDIES OF TUNGSTATE–TELLURITE GLASSES BY RAMAN SPECTROSCOPY AND DIFFERENTIAL SCANNING CALORIMETRY

I. SHALTOUT,† YI TANG,† R. BRAUNSTEIN† and A. M. ABU-ELAZM‡

†Department of Physics, University of California, Los Angeles, CA 90024, U.S.A.
‡Department of Physics, Faculty of Science, Al-Azhar University, Nasr City, Cairo, Egypt

(*Received* 27 *May* 1994; *accepted* 11 *August* 1994)

Abstract—Raman spectroscopy and differential scanning calorimetry (DSC) are used in this work to study lattice structures, crystallization behavior, effects of heat treatment and the thermal properties of a wide range of tungstate–tellurite glasses $\{(100-x)TeO_2 + xWO_3\}$ with $5 \leqslant x \leqslant 50$ mol%. We extended the glass formation range of this glass system up to 50 mol% of WO_3 using a platinum crucible. The Raman vibrational bands and the different coordination states of the constituent oxides are discussed. Interesting aspects of Raman spectra and DSC were found, and this gives integrated information about the short-range order of the structures of these glasses as a function of WO_3 concentration. The thermal parameters, such as the glass transition temperature (T_g), the onset of crystallization temperature (T_o), and the heat of crystallization δH were determined. The relation $\ln T_g = 1.6Z + 2.3$, where Z is some average coordination number of the constituent atoms, known for molecular and chalcogenide glasses, was found to be satisfied by these oxide glasses up to a certain threshold (27.5 mol%) of WO_3.

Keywords: A. glasses, A. oxides, C. differential scanning calorimetry (DSC), C. Raman spectroscopy, D. phonons.

1. INTRODUCTION

The first Raman study of tellurite glasses was reported previously for the glass system $(85TeO_2 + 15WO_3)$ [1]. Few Raman studies on tellurite glasses in general are found in the literature [2], and to the best of our knowledge the present work represents the first Raman study on a wide range of tungstate–tellurite glasses containing up to 50 mol% of WO_3. Infrared spectra and optical absorption spectra of the glass system (TeO_2–CaO–WO_3), as well as i.r. spectra and electron spin resonance spectra of the glass system $\{(100-x)TeO_2 + xWO_3\}$ with $0 \leqslant x \leqslant 33.8$ mol% have been reported in previous publications [3, 4]. The short-range order of the glass system $(80TeO_2 + 20WO_3)$ was discussed earlier on the basis of neutron diffraction techniques [5]. Tellurite glasses are technologically important since they are chemically stable, have high homogeneity and are resistant to divitrification at low temperatures ($T_g \approx 300$°C) [6]. Many binary and ternary tellurite glasses can be manufactured on a commercial scale with good reproducibility of optical constants; some applications of these glasses have been published [7–9]. The dipole–dipole correlation properties of the glass system $(77TeO_2 + 23WO_3)$ [10], the photochromism and electrochromism, and the space charge injection of some other tungstate glasses have been reported [11, 12].

These interesting properties of the tungstate–tellurite glasses motivated us to study the structures and crystallization behavior of a series of $\{(100-x)TeO_2 + xWO_3\}$ glasses with $5 \leqslant x \leqslant 50$ mol% using Raman scattering and differential scanning calorimetry (DSC) techniques.

2. EXPERIMENTAL ARRANGEMENTS

Reagent grade TeO_2 (Alfa Johnson Matthey Electronics, 99.995%) and WO_3 (Alfa Inorganic Ventron) were used to prepare the glass samples by fusing the mixtures of TeO_2 and WO_3 in a platinum crucible in a preheated furnace at 800°C for about 30 min to ensure complete homogeneity of the samples. For the glass system $\{(100-x)TeO_2 + xWO_3\}$ with $33 \leqslant x \leqslant 50$ mol%, the melting temperature was increased from 800 to 1000°C in order to obtain good quality samples. After complete fusion, the melt was quickly poured onto a stainless steel plate at room temperature. Bulk samples of about 2 cm diameter and 0.5 cm thickness were obtained, except for the sample with $x = 50$ mol% where only very small pieces (less than 0.5 mm in diameter and 0.1 mm in thickness) were obtained. The color of these glasses changed from yellow to light green to dark green as WO_3 concentration increased. The glassy state of all the samples was confirmed using X-ray diffraction techniques.

The Raman spectra were measured using a system consisting of a SPEX 1878 triplemate spectrometer, a Spectra Physics 2000 Argon laser operating at 5145 Å, and an RCA C31034 GaAs photomultiplier tube with a photon counting system. More experimental details can be found in Ref. [13]. The glass samples were used as castings where they have very good surfaces with high reflectivity. Initially, the Raman spectra were obtained for samples not subjected to any heat treatment or annealing processes and, subsequently, the Raman spectra were obtained for the same samples after different heat treatment processes.

For DSC measurements, glass samples were carefully ground in an agate mortar in order to avoid the effects of grain sizes on the results. Samples of about 0.01 g were used to avoid the temperature gradient through the sample. The scanning temperature was in the range of 0–600°C with a heating rate of 10°C min^{-1}. The measurements were carried out using a General V2.2A Dupont 9900 DSC system.

3. RESULTS AND DISCUSSION

Figure 1 shows the Raman spectrum of crystalline TeO_2 and WO_3, and the glass samples $\{(100-x)TeO_2 + xWO_3\}$ with $0.5 \leqslant x \leqslant 31.5$ mol%. The Raman frequencies of crystalline TeO_2 and WO_3, and the glass samples before and after heat treatment at 450°C for 18 h are summarized in Table 1. As can be seen in Fig. 1 and Table 1, the Raman bands of the glass samples have broadened and shifted to higher frequency values from that of crystalline TeO_2. This broadening could be related to chemical perturbation of the vibrational energies arising from glass former–glass modifier bonding. In the disordered matrix, the atoms are strained and have a distribution of bond angles, distances and orientations.

As can be seen in Fig. 1, the strongest sharp peak observed at 643 cm^{-1} in the Raman spectrum of crystalline TeO_2 (Fig. 1) has broadened and shifted to higher frequencies ($\sim$663 cm^{-1}) in the spectra of the glasses (spectra 1–5). This broadening, as mentioned above, is a result of the distribution of bond angles and average nearest-neighbor distances in the glass matrix. The strong peak at 663 cm^{-1} and the shoulder around 739 cm^{-1} spectrum 1 in Fig. 1 correspond to the vibrational oscillations of the TeO_4 tetrahedra in the glass matrix [14, 15].

It is known from the literature that TeO_2 has three different crystalline structures, the orthorhombic structure of D_{2h}^{15} symmetry and two tetragonal structures of D_4^4 symmetry (paratellurite) and D_{4h}^{15} symmetry (rutile), respectively [16]. The structural units are trigonal bipyramids with two O atoms in the axial position and the other two O atoms are in an equatorial position [17]. The trigonal bipyramids are deformed where the Te atom is not at the center of the equatorial plane and the third position in this plane is occupied with the free electron pair of the Te atom. The TeO_4 tetrahedra have axial symmetric vibration at $(A_1) = (^sTeO_2)_{ax} = 635$ cm^{-1} and equatorial symmetric vibration at $(A_1) = (^sTeO_2)_{eq} = 780$ cm^{-1} [18]. These frequencies appear in the Raman spectrum of crystalline TeO_2 at 643 and 761 cm^{-1}, respectively (Fig. 1).

Figure 2 shows an enlargement of the Raman spectra of crystalline TeO_2 and the $\{95TeO_2 + 5WO_3\}$ glass sample. The band at 663 cm^{-1} in the glass spectrum corresponds to the axial symmetric vibration of crystalline TeO_2 at 643 cm^{-1}, and the

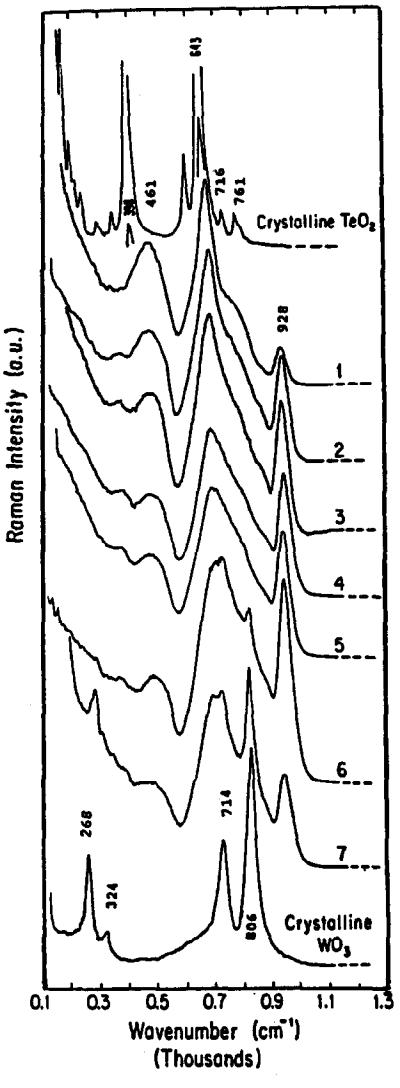

Fig. 1. Raman spectra of crystalline TeO_2, WO_3 and the glass system $\{(100-x)TeO_2 + xWO_3\}$ with $5 \leqslant x \leqslant 31.5$ mol%. (1) $x = 5$; (2) $x = 15$; (3) $x = 20$; (4) $x = 25$; (5) $x = 27.5$; (6) $x = 30$; (7) $x = 31.5$.

Table 1. Raman frequencies of crystalline TeO_2 and WO_3, the heated treated and untreated glass system $\{(100-x)TeO_2+xWO_3\}$

Sample	Raman frequency (cm^{-1})					Raman frequency (cm^{-1})				
Crystalline TeO_2:	187	230	283	334	398					
	587	643	716	761						
$(100-x)TeO_2+xWO_3$ glasses	Before heat treatment					Heat treated at 450°C for 18 h				
$x=5$			461_s	663_{vs}		261	328	388	590	639
	$(714–763)_{rsh}$			928_m				709	795	
$x=15$		353_{vw}	463_s	664_{vs}		263	324	390	594	640
	$(745–850)_{ush}$			925_m			675	709	795	911
$x=20$		353_{vw}	463_s	668_{vs}		262	323	388	591	637
	$(745–850)_{ush}$			925_{vs}				703	799	913
$x=25$		353_{vw}	460_s	668_{vs}		260	322	390	591	640
	$(745–850)_{ush}$			930_{vs}				700	800	910
$x=27.5$		354_{vw}	460_s	668_{vs}		262	326	391	590	635
	$(745–850)_{ush}$			930_{vs}				698	795	
$x=30$		353_{vw}	464_m	680_{vs}		262	328	383	590	639
	715_{ush}	805_s	930_{vs}				705	801	904	
$x=31.5$	268_m	353_{vw}	461_m	680_{vs}		260	324	383	590	638
	715_{ush}	805_s	929_m				704	801	910	
$x=33$	273_s	329_{vw}	462_{vw}	645_{sh}		269	333	391	591	646
	714_s	806_s	928_m				713	807	910	
$x=35$	273_s	325_{vw}	460_{vw}	645_{sh}		268	328	393	590	645
	714_s	806_s	928_m				709	808	913	
$x=40$	275_s	325_{vw}	460_{vw}	645_{sh}		268	329	392	590	646
	714_s	806_s	928_m				710	807	912	
Crystalline WO_3:	268	324	714	806						

m, medium; s, strong; rsh, resolved shoulder; sh, shoulder; ush, unresolved shoulder; vs, very strong; vw, very weak.

shoulder around 739 cm^{-1} is an envelope of the two weak bands at 716 and 761 cm^{-1} of crystalline TeO_2.

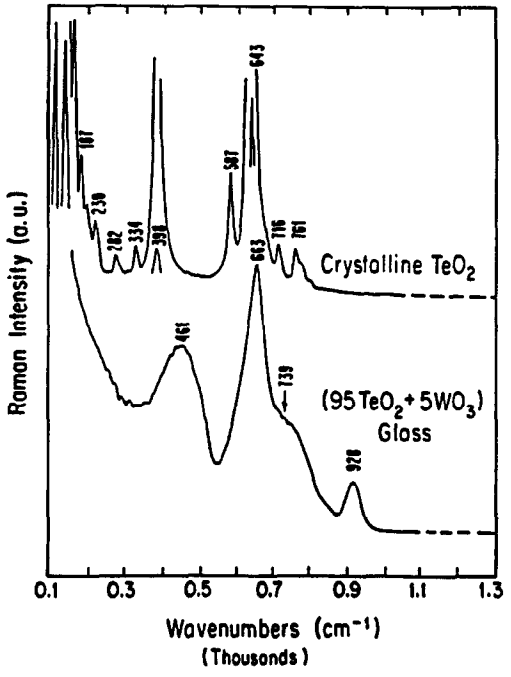

Fig. 2. Raman spectra of crystalline TeO_2 and the glass sample $\{95TeO_2+5WO_3\}$.

The Raman band at 663 cm^{-1} and the shoulder around 739 cm^{-1} are also i.r. active [19] and were detected around 662 and 774 cm^{-1} as shown in the i.r. spectrum of the $(95TeO_2+5WO_3)$ glass (Fig. 3).

As shown in Fig. 1, the peak at 663 cm^{-1} and the shoulder around 739 cm^{-1} gradually overlap as WO_3 concentration increases from 15 to 27.5 mol% (spectra 2–5). As WO_3 concentration reaches 30 mol% or more (spectra 6 and 7), the broad frequency envelope centered at 663 cm^{-1} splits into three bands which indicates a drastic structural change at these compositions.

As shown in Fig. 4(a), the crystallization temperature T_c, the glass transition temperature T_g and the onset crystallization temperature T_o reach a maximum as WO_3 concentration increases to 27.5 mol%. As shown in Fig. 4(b), the difference temperature $\delta T=(T_o-T_g)$, which represents the temperature interval during which nucleation and partial crystallization take place [20], and the heat of crystallization δH pass through a maximum at $WO_3=27.5$ mol%.

We now return to the assignment of the rest of the Raman peaks of the glasses shown in Fig. 1. The peaks around 460 cm^{-1} are due to the stretching vibrations of the bonds (Te–O–W) [14, 21, 22]. This represents the substitution of TeO_4 tetrahedra by WO_4 tetrahedra. Previous i.r. and neutron diffraction

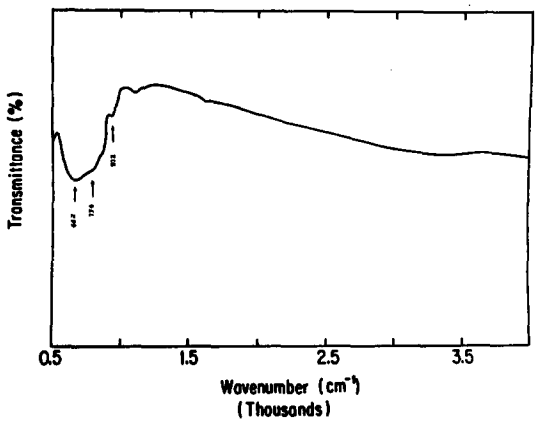

Fig. 3. Infrared absorption spectrum of the ($95TeO_2 + 5WO_3$) glass system.

studies [22, 23] showed such incorporation of the modifier cations in the glass matrix in various TeO_2-rich glasses. The bands around 928 cm^{-1} are due to the symmetric vibrations of WO_4 tetrahedra [24]. These bands were also observed around 932 cm^{-1} in the i.r. spectrum of ($95TeO_2 + 5WO_3$) (Fig. 3), which represents a typical spectrum of these glasses [19]. Dimitrov *et al.* [22] studied the i.r. spectra of the (TeO_2–WO_3) glass system and suggested a partial substitution of TeO_2 by WO_4 tetrahedra based on a similar band observed around 930 cm^{-1}. Also, Bobovish and Yakhind [23], in a Raman study of tellurite glasses, have detected this band around 930 cm^{-1}.

It is hard to judge the relative intensity of the bands around 461 cm^{-1} as a function of WO_3 concentration, since they overlap with the Rayleigh broad background or a cluster of low frequency optic modes. However, as shown in Fig. 1, it is clear that the relative intensity of the bands around 928 cm^{-1} increases with respect to the prominent band at 663 cm^{-1} as WO_3 increases from 5 to 30 mol%. Since the intensity of the Raman peak is proportional to the number of scattering units and their scattering efficiency (Raman cross-section), we may conclude that the number of WO_4 tetrahedra increases as WO_3 concentration increases and reaches a maximum at $WO_3 = 30$ mol% (spectra 1–6). Furthermore, we expect the formation of (Te–O–W) bonds, because both Te and W ions have comparable electronegativity values (2.1, and 2 respectively) and can therefore substitute for each other in bonding with O atoms. It is known that the density of tellurite glasses containing WO_3 increases as WO_3 concentration increases [25]; this density increase is due to the increase of WO_4 formation, which occupy a smaller space than WO_6 octahedra in crystalline WO_3.

Previous i.r. studies of TeO_2-rich glasses showed a band around 565 cm^{-1} which was ascribed to the (Te–O) vibrations where the O anions were considered as non-bridging oxygen (NBO) [26]. However, since we do not see this band either in the Raman or i.r. spectra [24] of our glass system, this may indicate that our glasses do not contain detectable NBO. It is well known that the glass structure is very sensitive to the melting temperature, the method of quenching, the crucible material and the thermal history.

Figure 5 shows the Raman spectra of crystalline WO_3 and the glass samples with $30 \leqslant x \leqslant 40$ mol%. For the two samples containing 30 and 31.5 mol% WO_3 (spectra 1 and 2), the two bands at 680 and 715 cm^{-1} correspond, respectively, to the axial symmetric vibration of TeO_4 tetrahedra in crystalline TeO_2 [$(A_1) = ({}^sTeO_2)_{ax} = 635\ cm^{-1}$] and to the band at 714 cm^{-1} of the WO_3 vibrations.

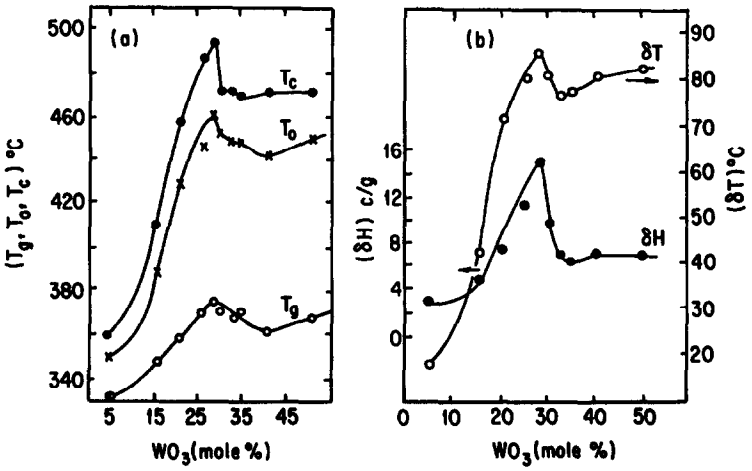

Fig. 4. (a) Glass transition temperature T_g, crystallization temperature T_c and onset crystallization temperature T_o. (b) Heat of crystallization δH and the gap $\delta T = (T_o - T_g)$ as a function of WO_3 concentration.

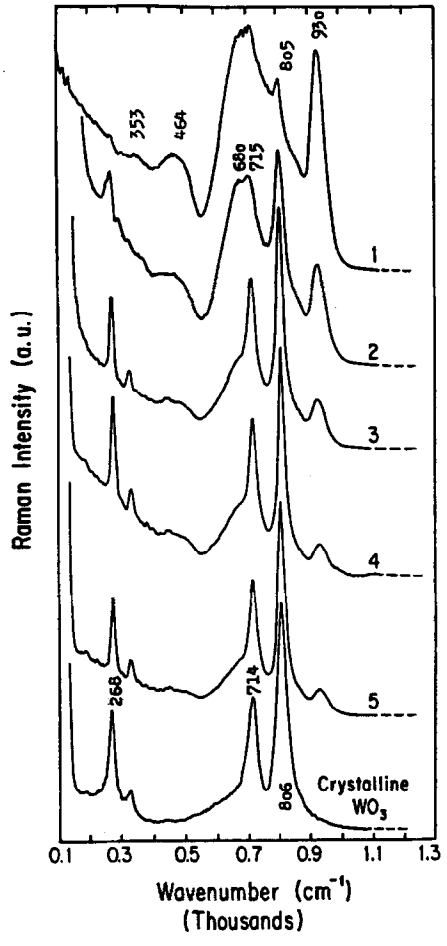

Fig. 5. Raman spectra of the glass system $\{(100-x)TeO_2 + xWO_3\}$ with $30 \leqslant x \leqslant 40$ mol%, and Raman spectrum of WO_3. (1) $x = 30$; (2) $x = 31.5$; (3) $x = 33$; (4) $x = 35$; (5) $x = 40$.

As shown in Fig. 5, the relative intensity of the bands around 930 cm^{-1} decreases continuously with respect to all other bands in each individual spectrum as WO_3 concentration increases above 30 mol%. Another peak is observed at about 805 cm^{-1}, which is not seen in the spectra of samples with $15 \leqslant x \leqslant 27.5$ mol% (Fig. 1, spectra 2–5). It is clear that the relative intensity of the two peaks at 805 and 715 cm^{-1} increases as WO_3 concentration increases and they correspond to the two peaks at 714 and 806 cm^{-1} of crystalline WO_3. Also, as WO_3 concentration increases the broad bands around 460 cm^{-1} gradually disappear and in addition a band around 265 cm^{-1} is observed and its relative intensity increases. All these observations indicate that the W ion coordination state changes from fourfold coordination with $5 \leqslant x \leqslant 30$ mol% (spectra 1–6 in Fig. 1) to sixfold coordination with $x \geqslant 31.5$ mol%, which is the coordination of W ions in crystalline WO_3 (spectra 2–5 in Fig. 6). Although W and Te ions have approximately the same electronegativity values, W ions possess a higher electronic polarizability (ionic charge/radius) than the Te ions. Thus, when $x \geqslant 31.5$ mol%, more oxygen can be attracted to W ions which in turn convert to octahedral coordination

In comparing the spectra in Fig. 1 and Fig. 6, it should be noticed that the structural entities of the dominant constituent oxide are present in the spectra of the glasses according to the content of each oxide. As we proceed from compositions of high WO_3 concentration to those of high TeO_2 concentration, we note a gradual broadening and overlapping of the respective bands. This reflects the gradual incorporation of the constituent polyhedra and complexes (TeO_4, WO_4, WO_6) forming the glass network. Also, it should be noticed that the Raman spectra of the glass samples with $33 \leqslant x \leqslant 40$ mol% are sharper than the spectra of the samples with $5 \leqslant x \leqslant 31.5$ mol%. The vibrational modes change when the oxygen bridges W and Te instead of two Te.

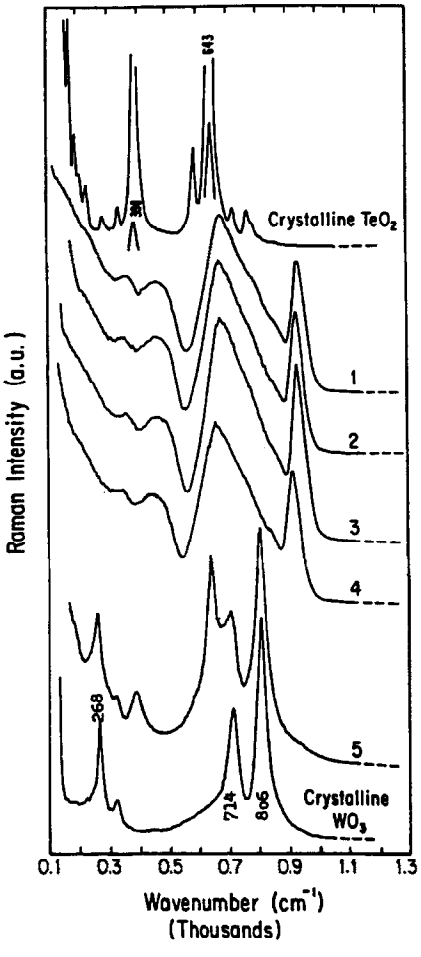

Fig. 6. Raman spectra of crystalline TeO_2, WO_3 and the glass system $(75TeO_2 + 25WO_3)$ before and after different heat treatment processes. (1) Untreated; (2) heat treated at 370°C for 90 min; (3) heat treated at 370°C for 21 h; (4) heat treated at 450°C for 30 min; (5) heat treated at 450°C for 18 h.

Hence the vibration of a TeO_4 tetrahedron depends on the number of O atoms (between zero and four) that are back-bonded to a W atom and vice versa for WO_4 tetrahedra.

From the analysis of the two classes of samples shown in Figs 1 and 5, respectively, we may conclude that as WO_3 concentration (x) increases, the number of WO_4 tetrahedra first increases to a maximum at $x = 27.5$ mol%, subsequently the number of WO_4 tetrahedra decreases and the number of WO_6 octahedra increases. For a variety of amorphous materials such change of the modifier ion coordination state as a function of composition has been reported [27–30].

To study the structural changes, nucleation, crystallization, and the thermal behavior of the samples, we measured the Raman spectra for the samples heat treated around both T_g and T_c for different periods of time. Figure 6 shows the Raman spectra of the glass sample ($75TeO_2 + 25WO_3$) as a representative one before and after different heat treatments, and the Raman spectra of both crystalline TeO_2 and WO_3. Spectrum 1 is the Raman spectrum of the untreated sample. Spectra 2 and 3 are the Raman spectra of the sample after heat treatment at 370°C for 90 min and 21 h, respectively. Spectra 4 and 5 are the Raman spectra of the sample after heat treatment at 450°C for 30 min and 18 h, respectively. Table 1 presents the positions of the Raman bands.

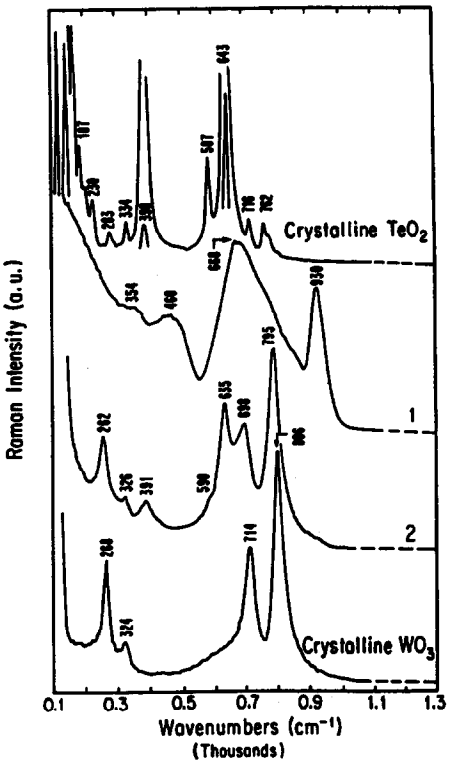

Fig. 8. Raman spectra of crystalline TeO_2, WO_3 and the glass system ($72.5TeO_2 + 27.5WO_3$) before and after heat treatment at 450°C for 18 h.

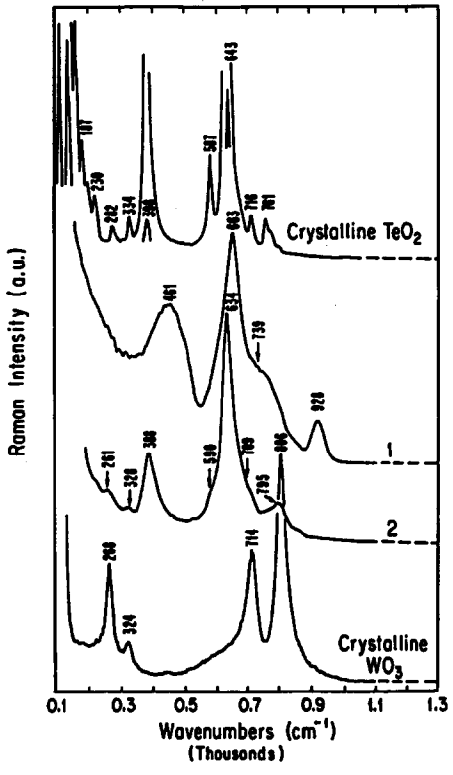

Fig. 7. Raman spectra of crystalline TeO_2, WO_3 and the glass system ($95TeO_2 + 5WO_3$) before and after heat treatment at 450°C for 18 h.

As shown in Fig. 6, spectra 2–4 look very much the same as the spectrum of the parent glass. This indicates that no partial crystallization or any ordered micro phases have developed upon heat treatment. That is because the heat treatment has been carried out for a short period at temperatures 370 and 450°C which are less than the crystallization temperature of the sample ($T_c = 488$°C). For the sample treated at 450°C for 18 h (spectrum 5), it is clear that it has been partially crystallized as a result of this heat treatment for a long time near the crystallization temperature. In the temperature range from T_c to T_g, the group of atoms have the translational energy to diffuse statistically and rearrange themselves in an ordered way to reduce the residual stress and reach a lower internal free energy, and consequently partial crystallization takes place.

Figures 7 and 8 show the Raman spectra of the glass samples ($95TeO_2 + 5WO_3$) and ($72.5TeO_2 + 27.5WO_3$), respectively, before and after heat treatment at 450°C for 18 h, and the Raman spectra of crystalline TeO_2 and WO_3. As shown in Fig. 7 spectrum 2, upon heat treatment two bands at 261 and 328 cm^{-1} emerge out of the broad background. The strong sharp band at 398 cm^{-1} of crystalline

TeO_2 reappeared in the glasses' spectra upon heat treatment at 388 (Fig. 7, spectrum 2) and 391 cm^{-1} (Fig. 8, spectrum 2), respectively, and the band at 587 cm^{-1} of crystalline TeO_2 reappeared as a weak shoulder around 590 cm^{-1} in both samples. The disappearance of the band around 460 cm^{-1} from both samples may indicate that the bonds (Te–O–W) have been broken as a result of the partial crystallization upon heat treatment. As shown in Fig. 8 spectrum 1, the broad band around 668 cm^{-1} splits into three bands at 635, 698 and 795 cm^{-1} (spectrum 2) upon heat treatment.

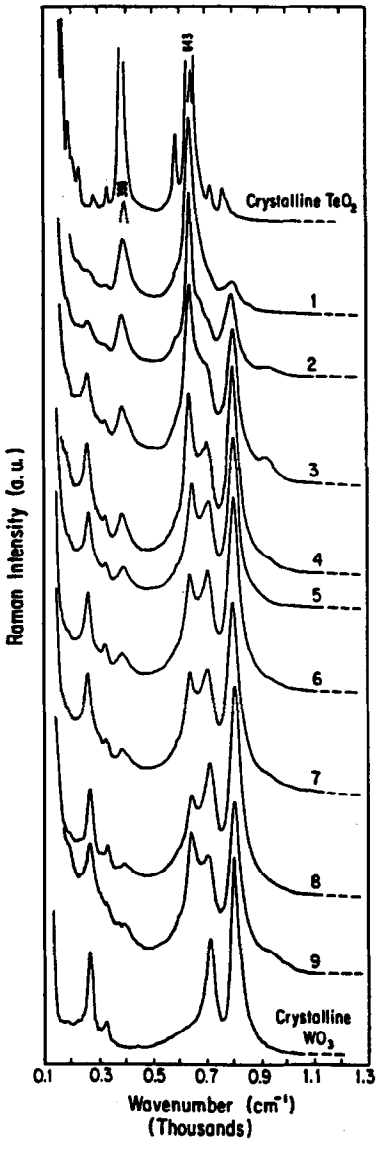

Fig. 9. Raman spectra of crystalline TeO_2, WO_3 and the glass system $\{(100+x)TeO_2+xWO_3\}$ with $5 \leqslant x \leqslant 35$ mol% after heat treatment at 450°C for 18 h. (1) $x = 5$; (2) $x = 15$; (3) $x = 20$; (4) $x = 25$; (5) $x = 27.5$; (6) $x = 30$; (7) $x = 31.5$; (8) $x = 33$; (9) $x = 35$.

The Raman frequencies of crystalline TeO_2 (summarized in Table 1) are characteristic of tetragonal TeO_2 of D_4 symmetry [16]. The characteristic Raman frequencies of the parent glasses, especially those with $5 \leqslant x \leqslant 27.5$ mol%, and the heat treated samples (Table 1) show a great correspondence to that of tetragonal TeO_2. Also, in the present work, as discussed earlier, certain modes of crystalline TeO_2 and the glass samples are active in both i.r. and Raman spectra (Table 1, Fig. 1, spectra 2, 7 and 8). On the other hand, the orthorhombic form of TeO_2 has no frequencies active in both Raman and i.r. spectroscopy [31]. These observations confirm the previously mentioned assignments of the different Raman bands and show that the TeO_2-rich glass structure is a disordered version of tetragonal TeO_2 where Te atoms are fourfold coordinated.

The spectra of all glass samples after heat treatment at 450°C for 18 h and the spectra of crystalline TeO_2 and WO_3 are compared in Fig. 9. As shown, the relative intensities of the band around 265 cm^{-1} and the very weak band at 328 cm^{-1} increase gradually as WO_3 concentration increases and their positions are about the same as the bands at 268 and 328 cm^{-1} of crystalline WO_3. Therefore, these bands correspond to vibrations of some tungstate complexes (WO_4 or WO_6 units) according to the concentration of WO_3. The relative intensities of the bands around 388 cm^{-1} and the shoulder around 590 cm^{-1} decrease as the WO_3 concentration increases and become very weak as WO_3 concentration reaches 40 mol%. These two bands have about the same positions as the strong band of TeO_2 at 398 cm^{-1} and the medium band at 587 cm^{-1}, and therefore they correspond to vibrational modes of TeO_2.

The very strong bands observed around 663 cm^{-1} in the spectra of the parent glasses (Fig. 1) have become more distinct and shifted to about 640 cm^{-1} (Fig. 9) after heat treatment. These bands, as we mentioned before, correspond to the axial symmetric $(^sTeO_2)_{ax}$ vibrational mode of TeO_2 at 643 cm^{-1}. Close to each of these bands a shoulder around 715 cm^{-1} is observed. It is clear that while the relative intensity of the bands around 640 cm^{-1} decreases continuously with the increase of WO_3 concentration (x), the relative intensity of the shoulders around 715 cm^{-1} increases and becomes a separated band at $x \geqslant 25$ mol%. The peaks around 928 cm^{-1} corresponding to the strong vibrations of the WO_4 units observed in the parent glasses spectra (Fig. 1) disappeared in Fig. 9. Finally a peak around 805 cm^{-1} (Fig. 9) is observed and its relative intensity increases very rapidly with the increase of WO_3 concentration. It is clear that the peak at 805 cm^{-1} corresponds to the band at 806 cm^{-1} of WO_6 vibrations in crystalline

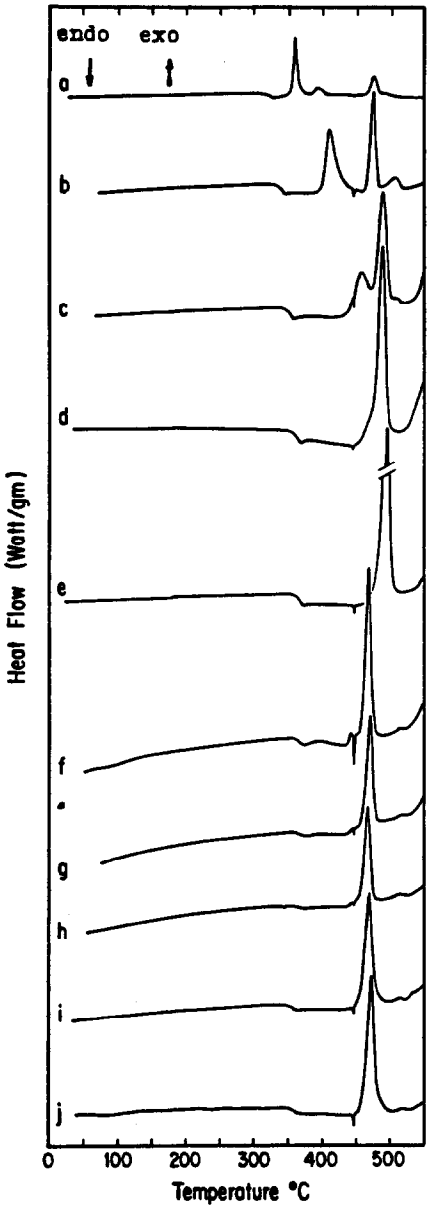

Fig. 10. Differential scanning calorimetry curves of the glass system $\{(100-x)TeO_2 + xWO_3\}$ with $5 \leqslant x \leqslant 50$ mol%. (a) $x = 5$; (b) $x = 15$; (c) $x = 20$; (d) $x = 25$; (e) $x = 27.5$; (f) $x = 30$; (g) $x = 31.5$; (h) $x = 33$; (i) $x = 35$; (j) $x = 50$.

WO_3 and this confirms the suggestion mentioned before for the parent glasses that the coordination of W ions is changing from four to six as WO_3 concentration increases.

In conclusion, upon heat treatment four bands at 265, 328, 715 and 805 cm^{-1} have been enhanced and their relative intensities increased with the increase of WO_3 concentration. Three other bands at 388, 590 and 640 cm^{-1} have also been enhanced and their relative intensities decreased with the increase of WO_3 concentration. All these observations confirm the suggestions mentioned before that the samples with $5 \leqslant x \leqslant 27.5$ mol% (Fig. 1 spectra 1–6) are similar in short-range order structure to crystalline tetragonal TeO_2, where Te atoms are tetrahedrally coordinated and the W ions are mostly fourfold coordinated. For the samples with $30 \leqslant x \leqslant 40$ mol% the W ions are sixfold coordinated.

Figure 10 shows the DSC curves of the glass samples $\{(100-x)TeO_2 + xWO_3\}$, where $5 \leqslant x \leqslant 50$ mol%. In general, the curves show a broad endothermic peak between 330 and 370°C which represents the glass transition temperature T_g. The thermal parameters estimated from these curves are collected in Table 2. These are: T_g, the glass transition temperature; T_c, the crystallization temperature which appears as a sharp exothermic peak; T_o, the onset crystallization temperature which is estimated by drawing tangents on the straight line portion of the crystallization peak; δH, the heat of crystallization obtained from the area under the crystallization peak; and finally $T = (T_o - T_g)$, which represents the temperature interval during which nucleation and partial crystallization take place [20]. As shown in curves a–c of Fig. 10, the samples containing 5, 15 and 20 mol% of WO_3 exhibit two successive crystallization peaks and the area under the peak depends on the composition. The two prominent successive crystallization stages may have resulted from the polymorphic nature of the tetragonal TeO_2 which can have either D_{4h}^{15} symmetry (rutile) or D_4^4 symmetry (paratellurite). One structure may crystallize first and then the other will crystallize at a higher temperature where the second crystallization peak is observed. Such a result of more than one exothermic peak or crystallization stages for these TeO_2-rich glasses is usually observed [32, 33]. After complete polycrystallization the final product may be mostly of tetragonal TeO_2 with some other tellurite–tungstate complexes distributed therein.

As shown in Fig. 10, for the samples with WO_3 concentration $x \geqslant 25$ mol% (curves e–j) only one crystallization peak is observed due to the higher content of WO_3 which may minimize the effect of the polymorphic nature of TeO_2 during the crystallization process and consequently result in simply crystallization behavior.

Tanaka [33] found that the simple relation $\ln T_g = 1.6Z + 2.3$, where Z is some average coordination number of the constituent atoms, is satisfied by a wide variety of molecular glasses, chalcogenices and organic polymers. A thermal study on a $\{35TeO_2 + (65-x)V_2O_5 + xFe_2O_3\}$ glass system reported earlier [34] showed that the same relation is followed by this glass system up to 10 mol% Fe_2O_3, after which deviation takes place. In the present

Table 2. Thermal parameters of the glass system $\{(100-x)TeO_2+xWO_3\}$

$(100-x)TeO_2+xWO_3$ glasses	T_g (°C)	T_o (°C)	δT $(=T_o-T_g)$ (°C)	T_c (°C)	Z	δH (°C g^{-1})
$x=5$	333	351	18	360, 393, 475	2.19	3.1
$x=15$	347	390	43	409, 476	2.22	4.53
$x=20$	359	430	72	458, 488	2.24	7.66
$x=25$	370	446	76	488	2.26	11.50
$x=27.5$	375	461	86	495	2.27	14.73
$x=30$	369	449	80	468	2.26	9.10
$x=33$	371	447	76	471	2.26	6.77
$x=35$	370	448	78	467	2.26	5.66
$x=40$	362	442	80	471	2.24	6.64
$x=50$	368	450	82	473	2.25	6.51

work, this relation is found to be satisfied as a function of WO_3 concentration up to 27.5 mol% and the deviation takes place when WO_3 concentration $x \geqslant 30$ mol%. This interesting behavior of these tungstate–tellurite glasses and the data from Ref. [34] suggest that this relation may turn out to be satisfied by a wide range of oxide glasses as well.

4. SUMMARY AND CONCLUSION

Structures, crystallization behavior and thermal properties of a wide range of tungstate–tellurite glasses have been studied using Raman spectroscopy and DSC. We have found that Raman and DSC analyses are two good complementary techniques to study the glass structure. The TeO_2-rich glasses containing $\geqslant 72.5$ mol% TeO_2 were found to be a disordered version of tetragonal TeO_2 where the Te atoms are fourfold coordinated. The number of WO_4 tetrahedra reaches a maximum at WO_3 concentration of 30 mol%, at which composition the sample reaches the percolation threshold and the WO_4 tetrahedra can link up. For the samples containing $31.5 \leqslant WO_3 \leqslant 40$ mol%, the W ions are in sixfold coordination and the number of WO_6 octahedra increases continuously as WO_3 concentration increases. We extended the glass formation range of the tungstate–tellurite glasses up to 50 mol% WO_3 using a platinum crucible where no contamination from the crucible can take place; however, no pure TeO_2 glasses could be obtained using a platinum crucible [35]. Previously, in the literature, pure TeO_2 glasses made by using alumina crucibles were found to contain between 1.5 and 6 mol% Al_2O_3 [16]. The structural changes due to composition and heat treatment have been studied using Raman spectroscopy, and the thermal parameters of the glasses have been estimated and discussed in terms of structural aspects. Finally, the relation $\ln T_g = 1.6Z + 2.3$ was found to be satisfied by these oxide glasses up to a certain percolation threshold of the modifier (27.5 mol% WO_3) after which deviation takes place.

Acknowledgements—This work was supported by the Ministry of Higher Education of the Arab Republic of Egypt, the Universitywide Energy Research Group of the University of California, and the State of California MICRO Program. The authors thank Mr B. Alavi for measuring the DSC and Dr E. R. Giessinger for stimulating discussions.

REFERENCES

1. Bobovish Y. O. and Yakhind A. K., *J. Struct. Chem.* **4,** 851 (1963).
2. Kneipp K., Burger H., Fassler D. and Vogel W., *J. Non-Cryst. Solids* **65,** 223 (1984).
3. Hogarth C. A. and Assadzadeh-Kashani E., *J. Mater. Sci.* **18,** 1255 (1983).
4. El-Zaidia M. M., Ammar A. A. and El-Mallawany R., *Phys. Status Solidi (a)* **91,** 637 (1985).
5. Kozhukharov V., Neov S., Gerasimova I. and Mikula P., *J. Mater. Sci.* **21,** 1707 (1986).
6. Greco E., Blair G. and Rindoge G., U.S.S.R. Patent 3690,908 co3c, 3/30 (1972).
7. Yakhkind A. K., *J. Am. Ceram. Soc.* **49,** 670 (1966).
8. Loffe B. V. and Yakhkind A. K., *Zap. Veses. Mineralog. Obshchestra* **94,** 475 (1965).
9. Yakhkind A. K. and Loffe B. V., *Optiko Mekhon. Prom.* **33,** 1 (1966).
10. Braunstein R., Lefkowitz I. and Snare J., *Solid State Commun.* **28,** 843 (1978).
11. Braunstein R., *Solid State Commun.* **28,** 839 (1978).
12. Braunstein R. and Bärner K., *Solid State Commun.* **33,** 941 (1980).
13. Abdelouhab R. M., Braunstein R. and Bärner K., *J. Non-Cryst. Solids* **108,** 109 (1989).
14. Kozhukharov V. S., Nokolov S. and Marinov M., *J. Mater. Res. Bull.* **14,** 735 (1979).
15. Nygrist R. A. and Kagel R. O., *IR Spectra of Non-organic Compounds.* Academic Press, New York (1971).
16 Lambson E. F., Saunders G. A., Bridge B. and El-Mallawany R. A., *J. Non-Cryst. Solids* **69,** 117 (1984).
17. Neov S., Grevassimova E. and Sydzhimov B., *Phys. Status Solidi (a)* **76,** 297 (1983).
18. Dimitriev Y., Dimitrov V. and Aranudov M., *J. Mater. Sci.* **18,** 1353 (1983).
19. Bahgat A. A., Shaisha E. E., Sabry A. I. and Eissa N. A., *Phys. Status Solidi (a)* **90,** K25 (1985).
20. Bahgat A. A., Shaisha E. E. and Sabry A. E., *J. Mater. Sci.* **22,** 1323 (1987).
21. Neov S., Gerassimova I., Krezhov K., Sypzhimov B. and Kozhukharov V., *Phys. Status Solidi (a)* **47,** 743 (1978).
22. Dimitrov V., Aranudov M. and Dimitriev Y., *Manatsh. Chem.* **115,** 987 (1984).
23. Bobovish Y. O. S. and Yakhind A. K., *J. Struct. Chem.* **4,** 851 (1963).

24. Shaltout I., Tang Yi, Braunstein R., Shaisha E. E. and Abu-Elazm A. M., to be published.
25. Shaisha E. E., Bahgat A. A. and Sabry A. I., *J. Mater. Sci. Lett.* **5,** 687 (1986).
26. Tarte P., *Silicate Ind.* **28,** 345 (1963).
27. Lyon R. J. P., *Nature* **196,** 266 (1962).
28. Lippincett E., *J. Res. natn. Bur. Stand.* **61,** 61 (1988).
29. Dachille F. and Roy R., *J. Am. Ceram. Soc.* **42,** 78 (1959).
30. Herzberg G., *Molecular Spectra and Molecular Structure.* VII Foreign Literature Press, Moscow (1949); second edn. Van Nostrand, Princeton, New Jersey (1950).
31. Hirashima Hiroshi, Michihisa I. and Yoshida T., *J. Non-Cryst. Solids* **86,** 327 (1986).
32. Ford N. and Holand D. H., *J. Glass Technol.* **28,** 106 (1987).
33. Tanaka K., *Solid State Commum.* **54,** 867 (1985).
34. Singh R., *J. Phys. D: Appl. Phys.* **20,** 1548 (1987).
35. Komatsu T., Tawarayama H., Mohri H. and Matusita K., *J. Non-Cryst. Solids* **133,** 105 (1991).